Metallophysics and Advanced Technologies
Металофіз. новітні технол.
Metallofiz. Noveishie Tekhnol.
2024, vol. 46, No. 9, pp. 833–844
https://doi.org/10.15407/mfint.46.09.0833
Reprints available directly from the publisher

PACS numbers: 61.50.Ks, 61.72.Hh, 61.72.Lk, 62.20.F-, 62.20.me, 81.40.Jj, 81.40.Np

Introduction of Crystallographic Factor into the Metal Fatigue Analysis

S. R. Ignatovych, M. V. Karuskevych, T. P. Maslak, O. M. Karuskevych, and T. V. Turchak*

National Aviation University,
1 Lyubomyr Huzar Ave.,
UA-03058 Kyiv, Ukraine
**G. V. Kurdyumov Institute for Metal Physics, N.A.S. of Ukraine,*
36 Academician Vernadsky Blvd.,
UA-03142 Kyiv, Ukraine

The discussed research combine two components: a) the improvement of the current procedure for stress–strain analysis of aircraft parts on the basis of the introduction of a crystallographic factor into the Huber–Mises–Hencky equivalent-stresses' calculation procedure; b) an example of application of this new calculation procedure into the practice of repairing aircraft skin that has been damaged by shooting, fatigue, corrosion, or firing.

Key words: metal fatigue, crystallography of slip, uniaxial loading, biaxial loading, equivalent stress.

Обговорювані дослідження поєднують дві складові: а) удосконалення наявної методики аналізи напруження–деформації деталів літака на основі упровадження кристалографічного фактора у процедуру розрахунку еквівалентних напружень Губера–Мізеса–Генкі; б) взірець застосування цієї нової процедури розрахунку в практиці ремонту обшивки літака, яку було пошкоджено стрілянням, втомою, корозією або обстрілом.

Ключові слова: втома металів, кристалографія ковзання, одновісне навантажування, багатовісне навантажування, еквівалентне напруження.

Corresponding author: Tetyana Petrivna Maslak
E-mail: tetiana.maslak@npp.nau.edu.ua

Citation: S. R. Ignatovych, M. V. Karuskevych, T. P. Maslak, O. M. Karuskevych, and T. V. Turchak, Introduction of Crystallographic Factor into the Metal Fatigue Analysis, *Metallofiz. Noveishie Tekhnol.*, **46**, No. 9: 833–844 (2024). DOI: 10.15407/mfint.46.09.0833

(Received 19 June, 2024; in final version, 20 August, 2024)

1. INTRODUCTION

Despite the increasing use of composites, metals continue to be the primary materials for the bearing components of aircraft and many engineering structure. Almost all operational loads of these engineering structures are fluctuating. Being applied thousands of times, they induce accumulation of fatigue damage, nucleation and propagation of cracks and failure. Generic mode of cyclical loads is multiaxial: proportional and disproportional, in-phase and out-of-phase. Fatigue damage assessment and failure prediction for this kind of fatigue is extremely challenging task. As the fatigue process depends on many factors, namely, parameters of loading, characteristics of metal, external conditions, *etc*., numerous methods for multiaxial fatigue analysis have been developed and currently are used.

Theories and corresponding calculation methods for the multiaxial fatigue analysis are classified as Stress-Based (Equivalent Stress approaches and Sines Method), Strain-Based (maximum principal strain theory, maximum shear strain theory, octahedral shear strain theory), and Energy-Based (plastic work per cycle, total strain energy density per cycle), as well as critical plane models. Comparative analysis of the contemporary methods are presented in the reviews [1–5] and other.

Considering the complex mechanism of development of a defect substructure in metals due to deformation processes [6], it is also worth noting the work of the authors [7] who assessed structure formation due to various types of deformation and showed that, far from thermodynamic equilibrium, synergistic structure formation plays an important role.

Unfortunately, there is no universal theory of the fatigue damage accumulation at the multiaxial cyclical loading and no approved and generally accepted method for fatigue life estimation; thus, any conclusion about correctness of the method for prediction the fatigue life must be checked by experiments.

The experiments conducted and described herein are aimed on the improvement of the efficiency of the multiaxial stress–strain analysis by the introduction of crystallographic aspects into the procedures of fatigue damage analysis for anisotropic materials.

Analysis of many structures subjected to the cyclical loading begins from the static strength calculations. For example, preliminary design stage for aircraft begins from the static stress–strain analysis and following assessment the geometry and dimensions of the aircraft parts, despite it is well known that aircraft are vulnerable to the cyclical loading rather than static. Many current practices of the stress–strain analysis begin from the assessment of the Huber–Mises–Hencky equivalent stresses. This classical approach works well for the ductile metals at static loading.

Huber–Mises–Hencky method was proved efficient tool not only for static loading, but also for fatigue analysis in many areas. For example, experiments and Finite Elements Analysis were performed for specimens modelling spot welded joints. Tensile-shear and cruciform-tension specimens' tests have shown that Huber–Mises–Hencky stress governs the fatigue failure of spot-welded joints. This criterion was successfully used for many bearing components and stress–strain conditions [8]. Another example deals with [9] fatigue life prediction of aircraft gun cabin structure under impact, caused by repetitive impact while firing, which causes vibration failure and structural damage.

The attempts to extend the Huber–Mises–Hencky approach by combining with contemporary critical plane theory exist and one of them was developed in the work [10] for out of face cyclical loading. The proposed criterion corresponds to the Huber–Mises–Hencky criterion modified by the coefficient taking into account the phase shift of stresses.

The Huber–Mises–Hencky formula for equivalent stress calculation does not consider crystallographic texture and following from that anisotropy of metals, caused, first of all by rolling. The accuracy of the calculations can be improved by introducing a crystallographic factor into the equivalent stress calculation. This was proved by testing aluminium alloy specimens subjected to combined tension-compression-torsion fatigue tests.

Out-of-phase fatigue loads are rather typical for all machines and mechanisms, but it is also well-known fact, that many of structures subjected to simpler in-phase loading. The one of the main reasons for planes accidents is pressurization of the aircraft fuselage. Examples of that are presented in Refs. [11, 12]. The pressurization cycles are in-phase. Many other examples of in-phase loading can be found for objects of machinery. These are objects where Huber–Mises–Hencky rule can be applied; moreover, this method can be improved by the taking into account the real crystallographic structure of the metallic parts.

2. MATERIALS AND METHODS

Aluminium alloys at present are widely used not only in aviation, but also in the automobile industry [13] and many others. In aviation industry, these are well known, high-strength alloys of Al–Cu–Zn–Mg (AA2xxx) group and Al–Zn–Mg–Cu (AA7xxx); in automobile industry, these are non-heat-treatable Al–Mg (AA5xxx) and the age-hardened Al–Mg–Si (AA6xxx) alloys.

Anisotropy of constructional metal is a result of their production process. Most pronouncing anisotropy resulted from the rolling texture. Preferable crystallographic orientation of grains is a main reason for Alclad alloys' plastic behaviour anisotropy [14].

Crystallographic anisotropy at fatigue was studied both on single crystals and on polycrystals. For single crystals, the crystallographic fatigue anisotropy can be explained by several aspects: a) by the level of shear stress in critical slip system; b) by the preferable mode of the slip, *i.e.*, easy slip or multiple slip with associated strain hardening; c) by the mutual location of the actuated slip planes and surface of the specimen.

For polycrystals, the influence of the grains crystallographic orientation also was found by many researches. In the work [15], for example it was stated that orientation of the grains determines peculiarities of dislocation structures and their evolution.

For aluminium used for clad layer of aluminium alloys the preferable orientation after the rolling {112}<111>, for core aluminium alloys, it is {110}<112> [16].

Metal fatigue phenomenon at the present time is considered as a result of dislocations motion along favourably orientated slip systems, their interaction, forming and evolution of defects structures. Tested in the presented experiments f.c.c. aluminium alloy has crystal lattice with twelve slip systems. Slip process depends mainly on the resolved shear stresses in slip systems, which in turn depends on the orientation of slip plane and slip direction relatively the load components. The orientation of actual slip systems influences the dislocation motion and fatigue damage, but this fact is not taking into account in conventional methods for the stress–strain analysis of parts subjected to the cyclical loading.

For many metals, the accumulation of fatigue damage accompanied

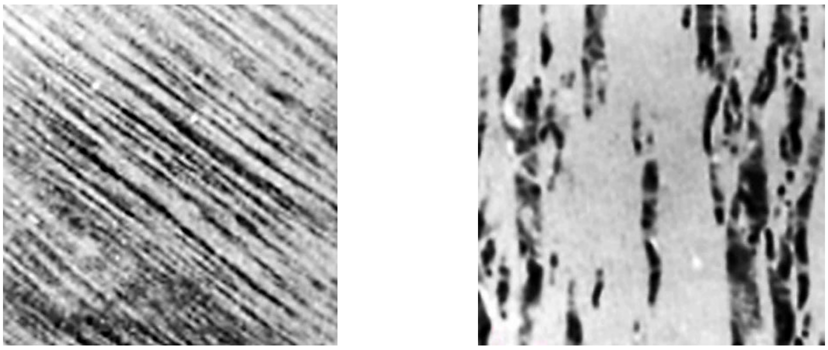

a *b*

Fig. 1. Deformation relief on the surface of aluminium single crystal: orientation <221>{110} (*a*); orientation <100>{100} (*b*) [17].

with formation of the surface relief. The surface deformation-relief sensitivity to the crystallography has been revealed both on single crystals [17] and on polycrystalline alloys. Surface relief on the aluminium single crystals is shown in Fig. 1. Examples of the surface relief observed on the surface of the polycrystalline D16AT specimens found at the process of cyclical loading are shown in Fig. 2. This phenomenon was revealed for D16AT, V95, 2024T3, 7075T6 alloys.

The intensity of the relief, expresses by the damage parameter D [18], evolves with number of cycles and correlates with consumed life of details. Damage parameter D reflects accumulated fatigue damage by the ratio of surface area with signs of extrusion/intrusion to the total observed surface area. Light microscope with magnification in the range from ×200 to ×400 may be efficiently use to get digital photo of the surface, while special software allows assessment of the damage parameter (Fig. 3).

Specimens made of Alclad aluminium alloy D16AT (analogues of 2024T3) where tested in the frame of conducted and partly presented here experimental research.

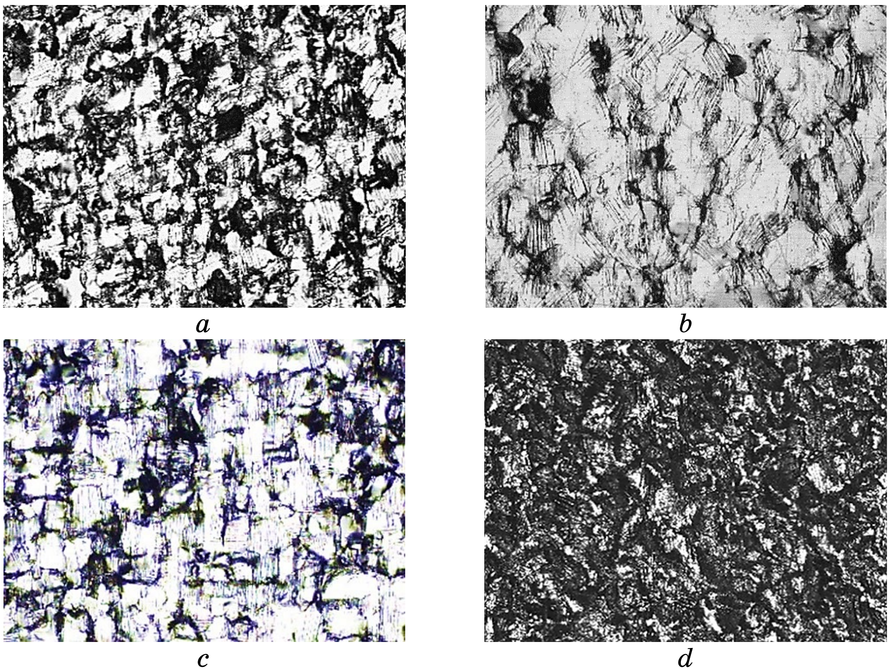

Fig. 2. Deformation relief formed under the action of cyclical loading: PRO_02 (5000) $\sigma_a = 118.7$ MPa, $\tau = 68.5$ MPa (*a*); TC_02 (5000) $\sigma_a = 150.0$ MPa, $\tau = 0$ MPa (*b*); TOR_03 (5000) $\sigma_a = 0$ MPa, $\tau = 150.0$ MPa (*c*); OP_03 (5000) $\sigma_a = 150.0$ MPa, $\tau = 86.0$ MPa (*d*).

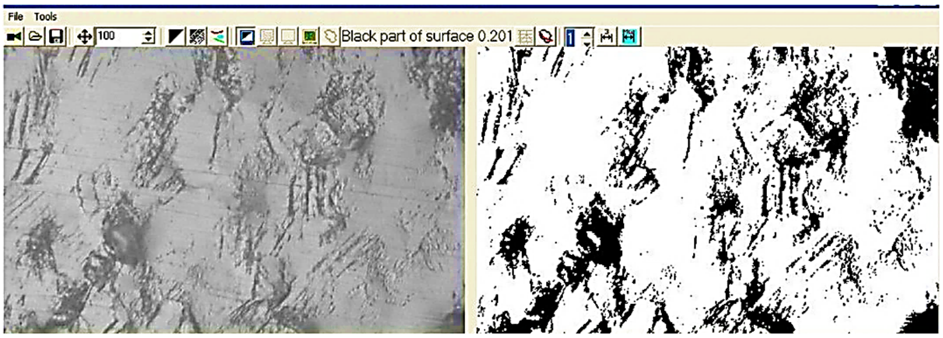

Fig. 3. Fragment of the damage parameter assessment: converting the initial photo of the deformation relief into the contrast image.

a

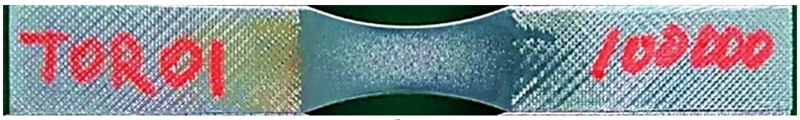

b

Fig. 4. Fragment of the damage parameter assessment: converting the initial photo of the deformation relief into the contrast image.

Distributions of the deformation relief on the surface of specimens after the 100000 cycles tested by tension–compression (Fig. 4, *a*) and torsion (Fig. 4, *b*) are shown below.

As it is was shown in the paper [19], relief pattern on the surfaces of the specimen tested under the different regimes of loading follow the distribution of the normal and shear stresses in the rectangular cross sections of specimens.

Works aimed on the improvement of the Huber–Mises–Hencky approach by the introduction of the crystallographic factor into the Huber–Mises–Hencky formula for equivalent stresses have been provoked by the observation of the surface deformation pattern, caused by the cyclical loads of some alloys. Crystallographic deformation relief reflects the accumulated fatigue damage as it was proved by the researches [17–20], thus the crystallography should be taken into account.

In Table 1, mechanical characteristics and chemical composition of the Alclad alloy D16AT as well as characteristics of its analogous alloy

TABLE 1. Mechanical characteristics and chemical composition of D16AT and 2024T3 [21].

Alloy	Ultimate tension strength, MPa	Yield strength, MPa	Elongation, %	Young modulus, MPa	Main components, %
D16AT	440.0	290.0	18	71.0	Cu—3.8–4.9 Mg—1.2–1.8 Mn—0.3–09
2024 T3	435.0	290.0	12	73.2	Cu—3.8–3.9 Mg—1.2–1.8 Mn—0.3–0.9

2024 T3 are shown [21].

3. CALCULATIONS

The introduction of the crystallographic factor into the procedure of the equivalent stresses assessment has been done by the following procedure: Step 1—assessment of the Schmid's factors for slip systems actuated by tension component; Step 2—assessment of the Schmid's factors for slip systems actuated by shear component; Step 3—Calculation of the resolved tension component by account of correspondent Schmid's factor; Step 4—Calculation of the resolved shear component by account of correspondent Schmid's factor; Step 5—Calculation of the corrected Huber–Mises–Hencky equivalent stress. For combined tension–torsion mode of biaxial loading, the formula

$$\sigma_{eq} = \sqrt{\sigma_x^2 + 3\tau_{xy}^2} \quad (1)$$

is transformed into

$$\sigma_{eq\,corrected} = \sqrt{(m\sigma)_x^2 + 3(m\tau)_{xy}^2}\,, \quad (2)$$

where σ_{eq} is equivalent Huber–Mises–Hencky stress, $\sigma_{eqcorrected}$ is equivalent Huber–Mises–Hencky stress corrected with account of crystallographic texture, m is Schmid's factor, σ_x is normal (axial) stress, τ_{xy} is shear stress.

Results of the calculation are presented in Table 2.

The relations shown in Figs. 6 and 7 confirm the relevance of the proposed method. For the specimens tested by the in-phase mode of loading, the relation between the number of cycles to failure and cor-

TABLE 2. Assessment of the Huber–Mises–Hencky stress with account crystallographic texture of tested specimens.

Mode of loading	Maximum normal component, σ_{max}, MPa	Maximum shear component, τ_{max}, MPa	Number of cycles to failure	Huber–Mises–Hencky stress, MPa	Schmid's factor for Slip systems actuated by the normal stress	Schmid's factor for slip systems actuated by the shear stress	Corrected Huber–Mises–Hencky stress, MPa
TOR 01	0	88.6	$23 \cdot 10^6$	150	0	0.24	36.83
TOR 03	0	150	266503	260	0	0.24	62.35
TC 01, $R=-1$	150	0	151355	150	0.45	0	67.5
TC 02, $R=-1$	150	0	181741	150	0.45	0	67.5
PRO, $R=-1$	106.05	61.24	420547	150	0.45	0.24	54.06
OP01	106.71	61.8	143070	151	0.45	0.24	54.45
OP02	149.99	86.61	48040	212	0.45	0.24	76.5

rected Huber–Mises–Hencky characterized by the $R^2 = 0.947$, but at the same time the correlation analysis reveals the reduction of the R^2 for the specimens tested at out-of-phase mode.

4. RESULTS AND DISCUSSION

New results of the deformation-relief monitoring carried out for the selected regimes of the uniaxial and biaxial loading are shown below in Fig. 5.

The following loading regimes have been provided: TOR—torsion; TC—tension–compression; PRO—proportional biaxial loading by tension–compression and torsion; OP—out-of-phase loading by tension-compression and torsion.

The obtained relations between the intensity of the deformation relief and percent of consumed fatigue life are combined regardless the level of stresses and mode of loading.

Deformation relief has crystallographic nature. Extrusion, intrusions, slip lines are the results of the dislocations motion along the crystallographic planes in the specific directions. Thus, the introduction of the crystallographic factor into the calculation of the stresses responsible on the fatigue damage looks reasonable.

Conclusion about possibility to improve accuracy of the fatigue

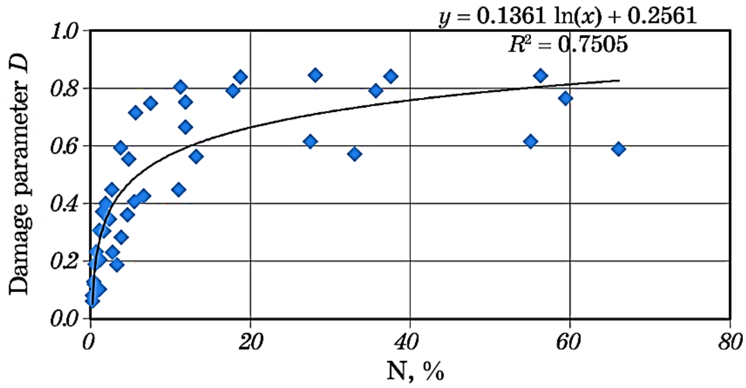

a

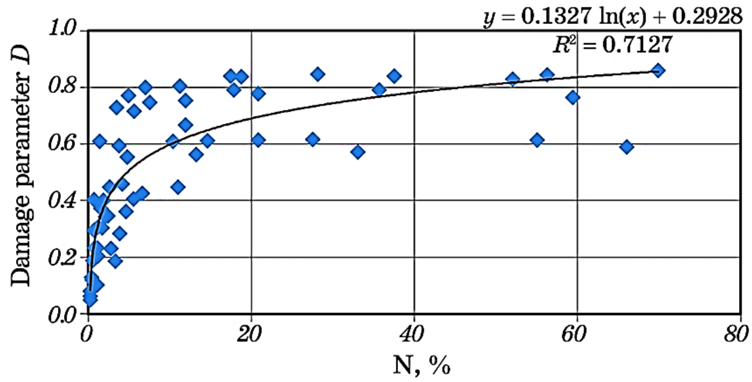

b

Fig. 5. Evolution of the surface relief intensity: without results of the out-of-face testing (*a*); with results of out-of-face testing (*b*).

analysis by the introduction of the crystallographic factor into the Huber–Mises–Hencky formula was made after the fatigue test with known texture. Some results of this experiment early were presented in the work [20].

The fatigue properties of materials are described by a SN-curve, thus correction of the equivalent stress assessment can be checked by the relevant correlation between the stress and number of cycles to failure.

Proposed technique for the introduction of the crystallographic factor into the Huber–Mises stress formula is less efficient for out-off-face loading. Figure 7 reveals the reduction of the correlation coefficient for the relation 'corrected Mises' stress–number of cycles to failure' when results of the out-of-face testing are used for the graph construction. Correlation coefficient drops from the 0.94 for in phase tension–compression and tension–compression–torsion modes to 0.831

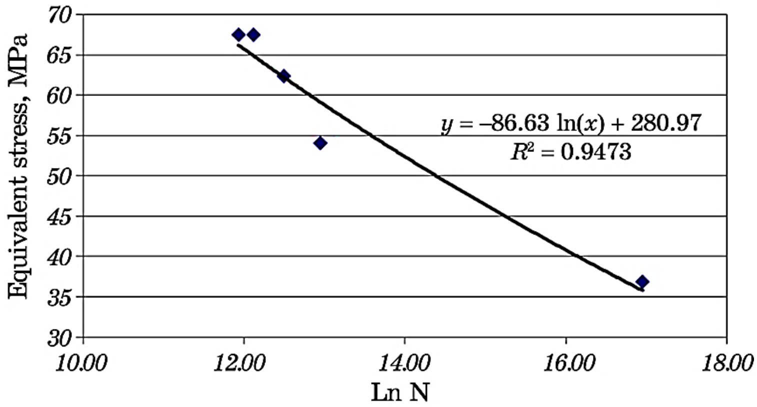

Fig. 6. Corrected Huber–Mises–Hencky stress–number of cycles to failure (only in-face loading results).

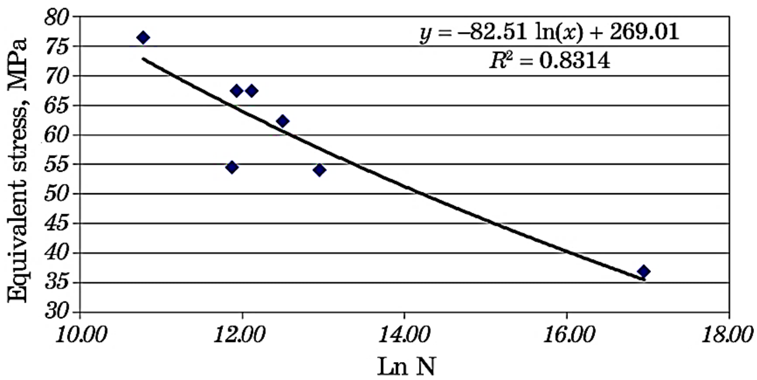

Fig. 7. Corrected Huber–Mises–Hencky stress–number of cycles to failure (out-of-face loading results are included).

for out-of-phase loading (Fig. 7).

Figure 8 illustrates the attempt to construct SN-curve on the base of Huber–Mises–Hencky formula for equivalent stress without respect to preferred crystallographic orientations of the grains of the investigated textured alloy.

As it is seen in Fig. 8, there is no correlation ($RI = 0.0415$) between the number of cycles to failure and conventional equivalent Huber–Mises–Hencky stress.

As an example of the practical application in aviation, the improvement of the aircraft skin repair can be considered. Fatigue, corrosion, denting, and even shooting, is a common type of in-service aircraft damage. These and other damages are repaired by patches or even by a

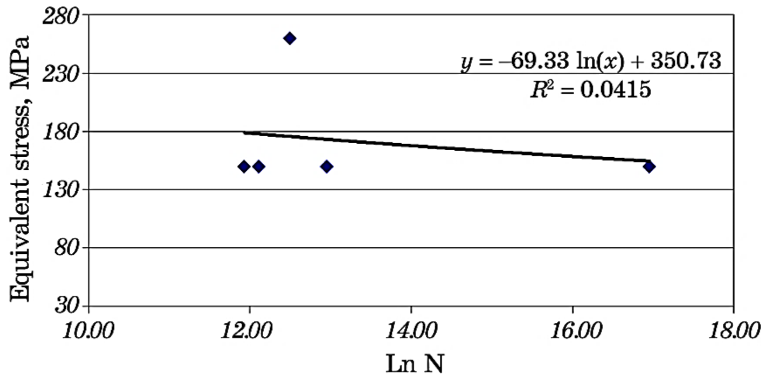

Fig. 8. Conventional equivalent Huber–Mises–Hencky stress–number of cycles to failure.

replacement of large panels. For aircraft parts made of metals, a similar material, for example the aluminium alloy 2024-T3 is used to make patches. This material, like all rolled metal sheets, is anisotropic.

Aircraft components, as well as repair patches, operate under multiaxial loading conditions. Fuselage constructions are subjected to bending, tension, compression, and pressurization loads. Patches installed at the different spots and integrated into the primary structure, withstand multiaxial loading. Since patches are made of anisotropic material, they must be oriented for better resistance to the loads to withstand actual loads. The enhanced procedure for Huber–Mises–Hencky equivalent stress calculation provides the possibility of minimizing equivalent stresses by optimally orienting the patch. As shown by preliminary fatigue tests, this may lead to a significant increase in the components' fatigue life.

5. CONCLUSION

Parts of many machines, mechanisms, constructions are made of anisotropic materials; this influences their bearing capacity. Static strength analysis of the components subjected to the multiaxial fatigue begins as a rule from the assessment of the equivalent uniaxial stresses, it is a routine procedure in current practice of aircraft preliminary and details design stage. The Huber–Mises–Hencky approach proposed many years ago still reliable tool for this task. Huber–Mises–Hencky method does not consider the anisotropy of constructional metals, thus the accuracy of the calculations can be increased by the introduction of crystallographic factor. This can be done for some materials by the taking into account their texture. To do this, normal and shear stresses' components of actual load are resolved to the actual crystallographic slip system; then, the equivalent stresses are found according to the generally excepted Huber–Mises–Hencky method. Experiments performed with specimens of Al–Cu–Mg alloy confirmed the proposed method.

Authors of the paper highly appreciate the support of the research team of Bydgoszcz University of Science and Technology (Poland), team leader Dr. Ł. Pejkowski, and hope to extend our collaboration in nearest future.

REFERENCES

1. A. Niesłony, M. Böhm, and R. Owsiński, *ICMFF12 MATEC Web of Conferences*, **300**: 15007 (2019).
2. Y.-Y. Wang and W.-X. Yao, *Int. J. Fatigue*, **26**: 17 (2004).
3. A. Carpinteri, A. Spagnoli, and S. Vantadori, *Fatigue Fract. Eng. Mater. Struct.*, **40**: 1007 (2017).
4. A. Karolczuk and E. Macha, *Int. J. Fract.*, **134**: 267 (2005).
5. https://www.diva-portal.org/smash/get/diva2:1576939/FULLTEXT01.pdf
6. E. Zasimchuk, T. Turchak, and N. Chausov, *Results Mater.*, **6**: 100090 (2020).
7. E. Zasimchuk, O. Baskova, O. Gatsenko, and T. Turchak, *J. Mater. Eng. Perform.*, **27**: 4183 (2018).
8. Y.-J. Yum, Y.-W. Chu, S.-J. Chu, J.-H. Kim, and H. You, *KSME International Journal*, **17**: 1113 (2003).
9. Zhenhao Ding and Ke Wang, *J. Phys.: Conf. Ser.*, **2472**: 012020 (2023).
10. M. Kuppers and C. M. Sonsino, *Fatigue Eng. Mater. Struct.*, **26**: 507 (2003).
11. https://www.faa.gov/lessons_learned/transport_airplane/accidents/G-ALYV
12. https://www.faa.gov/lessons_learned/transport_airplane/accidents/N73711
13. J. Hirsch and T. Al-Samman, *Acta Mater.*, **61**, Iss. 3: 818 (2013).
14. W. F. Hosford, *Mechanical Behavior of Materials* (Cambridge University Press: 2010), p. 419.
15. Dayong An and Stefan Zaefferer, *Proceedings of the 5th International Symposium on Steel Science: The Iron and Steel Institute of Japan (Nov. 13–16, 2017)* (Kyoto, Japan: 2017), p. 191.
16. G. Wasserman and I. Greven, *Textures of Metallic. Materials* (Moskva: Metallurgiya: 1969) (in Russian).
17. E. E. Zasimchuk, R. G. Gontareva, M. V. Karuskevich, I. K. Zasimchuk, and Yu. G. Gordienko, *Materials Structure & Micromechanics of Fracture. Conference Proceedings. MSMF-3* (Brno, Czech Republic: 2001), p. 232.
18. M. Karuskevich, O. Karuskevich, T. Maslak, and S. Schepak, *Int. J. Fatigue*, **39**: 116 (2012).
19. Ł. Pejkowski, M. Karuskevich, and T. Maslak, *Fatigue Fract. Eng. Mater. Struct.*, **42**, No. 10: 2315 (2019).
20. T. Maslak and M. Karuskevich, *Fatigue Fract. Eng. Mater. Struct.*, **46**, No. 3: 1211 (2023).
21. L. P. Luzhnikova, *Materialy v Mashinostroyenii. Tom. 1. Tsvetnyye Metally i Splavy* (Moskva: Mashinostroyenie: 1967).